*Macromolecules* **1991,** *24,* 3681-3688

# Adsorption Kinetics of Block Copolymers from a Good Solvent: A Two-Stage Process

**H. Motschmann and M. Stamm***

*Max-Planck-Institut für Polymerforschung, Ackermannweg 10, W-6500 Mainz, FRG*

**Ch. Toprakcioglu**

*Cavendish Laboratory, Madingley Road, Cambridge CB3 QHE, England, and Institute of Food Research, AFRC, Norwich NR4 7UA, England*

*Received November 6, 1990; Revised Manuscript Received January 31, 1991*

ABSTRACT: The adsorption kinetics and adsorption isotherm of a polystyrene (PS)-poly(ethylene oxide) (PEO) diblock copolymer onto a silicon wafer from toluene solution was measured in situ by ellipsometry. Both blocks are in good solvent conditions but the small PEO block is adsorbed while the much larger PS block dangles in solution. Thus, PS-PEO behaves like an end-adsorbed chain. The adsorption kinetics shows two processes on a clearly seperated time scale. In the beginning, the time behavior of the adsorbed amount can be described as a diffusion-controlled process leading to a surface coverage with small interaction between molecules. A still denser surface coverage is achieved by the penetration of chains through the existing monolayer combined with the conformational rearrangement to a more brushy conformation. Experiments with different molecular weights indicate that the repulsion between the nonadsorbing PS blocks determines the maximal adsorbed amount. The adsorbed monolayer can be rapidly and completely displaced by PEO oligomer with a length comparable to the PEO block in the block copolymer. Models of the adsorption process are discussed in detail.

## 1. Introduction

Adsorption phenomena on interfaces play an important role for many practical applications such as chromatography, adhesion,[1] stabilization of colloidal particles,[2] and biocompatibility of artifical organs in medicine.[3] For these reasons much effort has been devoted to clarifying the interfacial properties of polymer solutions in contact with a solid wall.

Polymer adsorption differs in significant ways from the adsorption of small molecules.

In contrast to small molecules, adsorbed polymers can adopt many different conformations. The conformations of isolated polymer chains as a function of the adsorption energy have been investigated by many authors and lead to the widely accepted loop-train-tail model.[4-9]

If one segment of the polymer is fixed to the surface, the adsorption probability for adjacent segments of the same molecule is increased, whereas for small molecules the adsorption probability of all molecules is equal. This should influence the adsorption kinetics.

Experimental methods to study adsorption processes should allow measurements in situ, since an adsorbed polymer film can be regarded as a concentrated polymer solution and hence its behavior is also determined by the solvent. Beside other optical methods like surface plasmon spectroscopy, ellipsometry allows the study of adsorption processes with a sufficient time resolution. Ellipsometry is an optical method, which uses the fact that the state of polarization is changed during reflection when the substrate is covered by an adsorbed film. On the basis of model calculations one obtains information on the optical thickness (adsorbed amount) of the film. In optimized cases a separate determination of the refractive index and the layer thickness is possible.

We use a recently constructed, self-built null ellipsometer to measure the adsorption kinetics and isotherm of a diblock copolymer of polystyrene (PS) and poly(ethylene oxide) (PEO) from toluene onto an oxidized silicon wafer. Toluene is a solvent for both blocks and no micellization occurs. The adsorption behavior should therefore be dominated by the interaction strength between each block and the surface. From the chemical point of view one can expect that the polar PEO block shows a stronger attraction to the $SiO_2$ surface than the unpolar PS block. Since the length of the PEO block in the polymer used is small compared to the PS block our system is expected to simulate end-attached polymer chains, which have attracted the attention of various theoretical groups, who made predictions about the adsorption process and the concentration profile.[10-12]

In particular, two regimes are predicted: a first regime with a largely unperturbed chain conformation at the surface ("mushroom" conformation) and a second regime at larger surface coverage with a brushlike conformation of adsorbed chains. Conformations and density profiles in this case of end-adsorbed chains are quite different from, e.g., homopolymer adsorption, since the chain is ideally only attached at one point to the surface while the other part does not adsorb.

Theories have been recently extended to also include kinetic effects.[23] Two time regimes of adsorption are predicted starting from a diffusion-limited regime at short times and changing to a regime at longer times where the penetration of the chains through an activation barrier formed by the already adsorbed chains is considered. A distinct crossover between the regimes is expected.

Experiments are, however, mostly performed in the static limit. It is shown for instance by force balance measurements[14] that terminally attached PS chains form a brushlike conformation. This is obtained both from a model fit to the force-distance profile and from the large distance for the onset of interaction. This technique, however, is less suitable for the study of adsorption isotherms or the kinetics of adsorption. Polymers used in this study[14] are actually identical with those used in our experiments. Using two techniques, we might get a more detailed picture of the adsorption process.

The time dependence of the adsorption process of PS-PVP block copolymers has recently been investigated by a surface plasmon technique.[24] The kinetics of adsorption

0024-9297/91/2224-3681$02.50/0 © 1991 American Chemical Society

**Table I**
**Molecular Characteristics of the Used Polymers**[a]

| sample | $M_w$ | $M_w/M_n$ | wt % PEO | $(PS)_x$ | $(PEO)_y$ | origin |
|---|---|---|---|---|---|---|
| PS | 192 000 | 1.04 | 0 | 1846 | | PSS |
| PS–PEO-80 | 80 000 | 1.08 | 5 | 730 | 90 | Pol. Lab. |
| PS–PEO-184 | 184 000 | 1.10 | 4 | 1700 | 167 | Pol. Lab. |
| PS–PEO-502 | 502 000 | 1.13 | 0.8 | 4788 | 91 | Pol. Lab. |
| PEO | 8 500 | 1.2 | 100 | | 91 | Fluka |

[a] PS, polystyrene; PEO, poly(ethylene oxide); PS–PEO, diblock copolymer of PS and PEO. The percentage of PEO was determined by NMR spectroscopy.

differs quite significantly for different concentrations. This is in this case mostly an effect of micelle formation at higher concentrations, but the adsorption rate is in all cases far below the diffusion limit. Similar results are reported for PS–PEO block copolymers adsorbed from a selective solvent, cyclopentane.[25] Adsorption again strongly depends on concentration and is much faster above the critical micelle concentration. Two time regimes are observed, at short times a transport limited and at longer times a logarithmically slow process.

In the present study we investigate PS–PEO block copolymers of different molecular weights where both blocks are in good solvent conditions. Micelle formation is thus generally not observed, while the PEO block still acts as an anchoring block to the wafer surface. A serious problem for ellipsometry is the small contrast between solution, adsorbed polymer film, and silicon oxide substrate. The experiments are, however, still very sensitive to the amount of block copolymer adsorbed to the surface while the film thickness is much more difficult to obtain. We will first describe our experimental setup. Besides ellipsometry, additional dynamic light scattering and force balance measurements are performed. Adsorption kinetics is followed as a function of concentration and molecular weight, keeping the size of the PEO anchoring block approximately constant. Results are discussed with respect to detailed kinetic and static model descriptions for the adsorption of end-functionalized polymer chains.

## 2. Experimental Section

**2.1. Materials.** The molecular characteristics of the polymers used are given in Table I.

Mirror polished silicon wafers with a well-defined oxide layer (typically 20 and 1500 Å), which were kindly supplied by Wacker Chemie, are used as substrates. The surface roughness was characterized by phase measurement microscope interferometry and found to be less than 10 Å. In order to obtain reproducable results the following cleaning procedure is necessary: (1) 15-min ultrasonic bath with chloroform, (2) 15-min ultrasonic bath with acetone, (3) overnight in an oxidizing 1:1 mixture of $NH_3$ and $H_2O_2$, (4) rinsing with triply distilled water, and (5) drying with nitrogen free of dust.

The solvent toluene (p.A. quality) was filtered through a Millipore filter before use to remove dust. Most of the adsorption runs were carried out with toluene freshly distilled over Na, although no significant changes occurred with undried toluene. Experiments were performed with a polymer concentration up to 0.15 mg/mL. Since it is known that PS–PEO block copolymers form micelles in cyclopentane, which is, however, a much worse solvent for both blocks, we checked micelle formation for our studies by dynamic light scattering. The apparatus used and data analysis are described elsewhere.[22] Experiments were performed up to a concentration of 5 mg/mL in toluene, much higher than the concentrations used during the ellipsometric adsorption experiments. There was no evidence for micelle formation under those conditions. We obtained from the dynamic light scattering data proof of the very monodisperse size distribution and a hydrodynamic radius of $R_h$ = 100 Å for PS–PEO-184. This is consistent with literature data for the homopolymer PS of similar molecular weight.

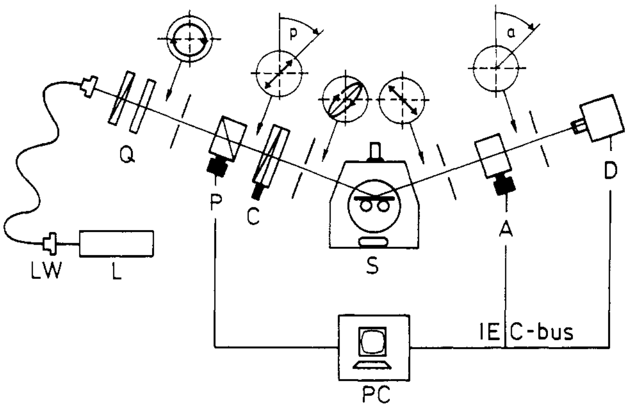

**Figure 1.** Schematic experimental set up. Key: LW, single-mode wave guide; L, He–Ne laser, Ar laser; Q, polarizer and quarter-wave plate to produce circular polarized light; P and A, polarizer and analyzer mounted in rotable goniometers driven by stepping motors; C, Soleil-Babinet compensator; S, cell with sample-holding device and thermostat circulation, windows at 70°, tightened via a Teflon-coated O-ring, magnetic stirrer, mounted on a tiltable $z$ translation; D, photomultiplier with digitial multimeter. The state of polarization of the light after the various optical components is indicated in the top. The measurements are performed in such a way that the elliptically polarized light caused by polarizer and compensator is changed during reflection at the sample to linear polarized light and is extinguished by the analyzer.

**2.2. Ellipsometry.** The measurements are performed using a self-built computer-controlled null ellipsometer in a vertical polarizer compensator sample analyzer (PCSA) arrangement (Figure 1).

The polarizer and analyzer are made of Glan-Thompson prisms with an extincion of $10^{-6}$ (Drs. Steeg and Reuther). The prisms are mounted in accurate rotatable goniometers (PI) and driven by stepping motors. As a compensator we use a Soleil-Babinet with an adjustable phase retardation and an accuracy of 0.001 $\lambda$ (Drs. Steeg and Reuther). The fast axis of the compensator is fixed at 45.00° to the plane of incidence. Light is detected by a red-sensitive photomultiplier (Hamamatsu R928), current to voltage conversion circuit, and a fast integrating digital multimeter (Prema).

The polarizer is adjusted in such a way that the elliptically polarized light caused by the compensator is changed after reflection to linear polarized light and can be extinguished by the analyzer. The state of polarization of the light when it passes each optical component is indicated in Figure 1.

The exact extinction settings of polarizer and analyzer are determined by measuring the parabolic position–intensity signal near the minimum. It is important to determine first the exact extinction position for the polarizer, since the signal for the analyzer is only a parabola for polarizer settings close to the minimum. The measurements are automated by a computer via an IEC bus and a stepping-motor control unit.

The ellipsometric angles $\Delta$ and $\Psi$ were obtained by the polarizer $p$ and analyzer $a$ settings with respect to the plane of incidence: $\Delta = 2p + 90$ and $\Psi = a$.[13] $\Delta$ and $\Psi$ were determined by taking the average of zone I and zone III.[17] The differences among the ellipsometric zones are usually less than 0.2°. We use a single-mode fiber (Schott) to have the capability of carrying out spectroscopic measurements using different lasers without new alignment of the angle of incidence. All measurements described here were performed with a He–Ne laser with a wavelength of 632.8 nm. The angle of incidence can be changed mechanically by goniometers and was fixed to 70.00°. All angles are reproducable within an accuracy of 0.01°.

Adsorption runs are performed as follows: The freshly cleaned silicon wafer is placed in a specially built trapezoidal glass cell (Hellma). The windows are largely stress free. Differences in the ellipsometric angles $\Delta$ and $\Psi$ in the cell compared to those in air were found to be within the experimental accuracy of 0.01°.

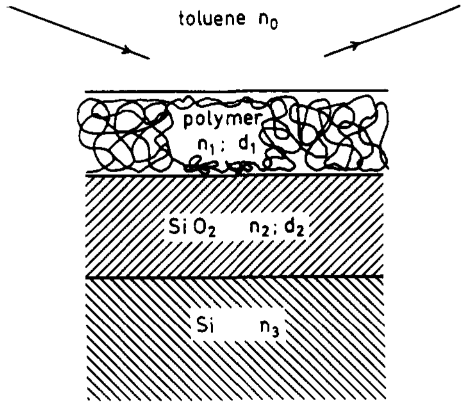

**Figure 2.** Layer model of an adsorbed homogeneous polymer layer on a silicon wafer used for data interpretation. The measured refractive index of $SiO_2$ is $n_2 = 1.460$, of Si is $n_3 = 3.858 - i0.018$, and of toluene is $n_0 = 1.4926$ ($\lambda = 633$ nm). $d_1$ and $d_2$ are the layer thicknesses of the polymer and $SiO_2$ layer, respectively. Only $n_1$ and $d_1$ are model parameters during adsorption of the block copolymer on silicon.

The cell is filled with toluene through a Millipore filter and kept at a constant temperature of 20 ± 0.05 °C by a thermostat. The constancy of the ellipsometer readings with time is checked. Then the polymer, dissolved in toluene, is injected and the solution is stirred for a period of 3 min. Every 11 s a pair of ellipsometric angles is recorded.

**2.3. Data Analysis.** Data are analyzed by assuming a homogeneous layer for the polymer film (Figure 2). The refractive index $n_1$ and the layer thickness $d_1$ were determined from the basic equation of ellipsometry:[13]

$$\tan \Psi e^{i\Delta} = \frac{R_p^{\text{all}}}{R_s^{\text{all}}} = f(n_0,n_1,d_1,n_2,d_2,n_3,\lambda,\phi) \qquad (1)$$

$R_s^{\text{all}}$ and $R_p^{\text{all}}$ are the complex overall reflection coefficients for eigenpolarization both parallel and perpendicular to the plane of incidence. They are a function of the (complex) refractive indexes of all media, the layer thicknesses, the wavelength $\lambda$, and the angle of incidence $\phi$. Because of the nonlinear and transcendental nature of eq 1, it is impossible to determine the unknown film parameters $n_1$ and $d_1$ directly. We use the following numerical iterative procedure:

Starting with a reasonable value for the refractive index $n_1$ of the adsorbed polymer layer, the Fresnel reflectivity coefficient for each interface can be determined. With the known thickness of the silicon oxide the complex overall reflectivity coefficient of the silicon and silicon oxide can be determined by means of the matrix technique,[15] using the fact that the tangential components of the electric and magnetic field have to change steadily at each interface. Equation 1 can then be simplified to a complex quadratic equation for the unknown film thickness $d_1$. Since the starting value of $n_1$ is not the true refractive index of the film, the solution of this equations leads to a complex film thickness $d_1$. The imaginary part of $d_1$ is minimized by systematic variation of $n_1$. This iterative cycle ensures that the experimental data are fitted within the experimental scatter to the adopted layer model. The measured refractive index of the silicon was $n_3 = 3.858 - i0.018$, the refractive index of the silicon oxide was $n_2 = 1.460$.

The amount of the adsorbed polymer $A$ (mg/m$^2$) was calculated by use of the following equation:

$$A = d_1(n_1 - n_0)/(\mathrm{d}n/\mathrm{d}c) = d_1c_1 \qquad (2)$$

$d_1$ is the calculated layer thickness and $n_1$ is the refractive index of the adsorbed film; $n_0$ is the refractive index of the pure toluene and d$n$/d$c$ is the refractive index increment of PS–PEO in toluene. It has been determined on an Abbe refractometer to be d$n$/d$c$ = 1.020 × $10^{-4}$ mL/mg. $c_1$ is the average polymer concentration in the layer.

**2.4. Model Considerations.** Since the refractive index of the adsorbed polymer layer is close to the refractive index of pure toluene, a separate determination of $n_1$ and $d_1$ is difficult. A set of ellipsometric angles $\Delta$ and $\Psi$ can be produced within the experimental accuracy of 0.01° by using a higher refractive index $n_1$ and a lower thickness $d_1$ or reverse. The product of $n_1d_1$ turns out to be an invariant quantity for the adopted layer model (Figure 2) with a homogeneus polymer layer.

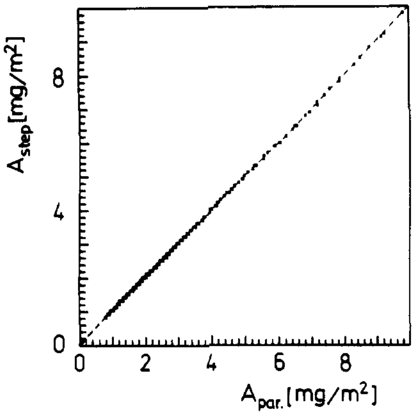

**Figure 3.** Adsorbed amount $A_{par}$ from a parabolic segment–concentration profile in comparison to the adsorbed amount for a step profile $A_{step}$. Each point corresponds to a set of $\tilde{n}$ and $\tilde{k}$ of a parabolic profile $A_{step}$. $n(z) = \tilde{n}(1 - \tilde{k}z^2) + n_0$. The parameters $\tilde{n}$ and $\tilde{k}$ were varied in the range $\tilde{k} = [1 \times 10^{-6}–2.5 \times 10^{-5}]$ and $\tilde{n} = [0.006 - 0.02]$ in a systematic manner. The adsorbed amount $A_{par}$, and the ellipsometric angles $\Delta$ and $\Psi$ corresponding to this profile, are calculated. $\Delta$ and $\Psi$ are then analyzed by a step function profile in the same manner as the experimental data. The calculated adsorbed amount $A_{step}$ from the step function data are identical with the adsorbed amounts $A_{par}$ of the parabolic profile within a scatter of 0.05%.

There are several theoretical predictions for concentration profiles of end-attached polymer chains. It is obvious that the assumed step function based on the scaling theory of Alexander[10,11] is only a very crude description of the true segment concentration of the adsorbed polymer layer. More advanced studies are the mean field calculations of Millner et al.,[12] which predict a parabolic concentration profile. It turns out that the assumptions made for these calculations are the closest to our experimental results.

Dolan and Edwards[16] carried out Monte Carlo simulations based on a random flight model that takes excluded volume effects into account. The derived profile shows a maximum close to the surface, which slowly decays to zero.

To check the dependence of the adsorbed amount on the used model, we carried out computer simulations. For instance, we assumed a parabolic refractive index profile corresponding to the theory of Millner.

$$n(z) = \tilde{n}(1 - \tilde{k}z^2) + n_0 \qquad (3)$$

This profile is characterized by the parameters $\tilde{k}$ and $\tilde{n}$, where $\tilde{k}$ determines the layer thickness and $\tilde{n}$ the refractive index at the surface; $n_0$ is the refractive index of pure toluene. We approximated the profile by 100 single-step functions using a variable-step width varying with the slope. Then we calculated the ellipsometric angles $\Delta$ and $\Psi$ and the adsorbed amount. By variation of the parameters $\tilde{n}$ and $\tilde{k}$ we obtain a set of angles $\Delta$ and $\Psi$, which were interpreted in the same manner as the experimental data; i.e., they were analyzed on the basis of the step function profile. The result is given in Figure 3, where each point corresponds to a given parabolic profile with a well-defined adsorbed amount of $A_{par}$ plotted via the calculated adsorbed amount of the step function $A_{step}$.

The simulations reveal that the adsorbed amount as determined from a model fit to ellipsometric data is independent of the profile used for the adsorbed layer. This statement is valid for all mentioned profiles. Even the data for an exponential profile show very little deviation from the step data. From ellipsometic data (of one wavelength) it is thus not possible to obtain information on the nature of the profile of the absorbed polymer layer.

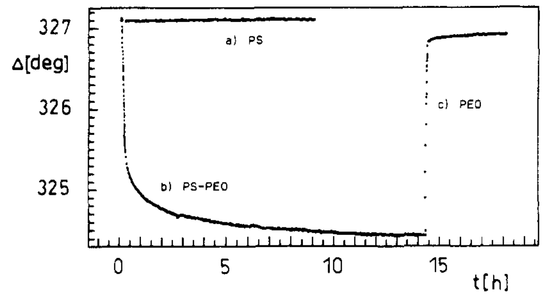

**Figure 4.** Ellipsometric angle Δ versus time. With a pure PS solution ($c = 0.03$ mg/mL; Figure 4a) the ellipsometric angle Δ does not change with time, whereas the block copolymer PS–PEO-184 ($c = 0.015$ mg/mL; Figure 4b) is adsorbed, as indicated by a decrease in Δ leading to a final plateau value. The adsorbed layer can be rapidly displaced by PEO oligomer ($c = 0.015$ mg/mL; Figure 4c).

## 3. Results

Figure 4 shows a typical measurement of the ellipsometric angle Δ revealing all qualitative features of the adsorption runs.

If one injects only the homopolymer PS at a concentration of 0.03 mg/mL into the cell, no changes in the ellipsometric angles occur (Figure 4a). Thus, we conclude that under the conditions used the homopolymer PS does not adsorb from toluene onto silicon oxide. This is in agreement with earlier studies of Taunton et al.[14,26] using the force balance technique.

As soon as the diblock copolymer PS–PEO of comparable molecular weight to the PS homopolymer is added (Figure 4b) a decrease in Δ occurs, indicating a growing layer. Thus, one can conclude unambiguously that the PS–PEO block is anchored through the small PEO block at the wafer surface. Both blocks are in good solvent conditions and no micellization occurs, which is evident from our dynamic light scattering data. In this sense the block copolymer behaves like a homopolymer PS of similar molecular weight with only an end-functionalized group at one end, which favors adsorption to the surface. Recently, Cogan and Gast[18] reported the formation of micelles for a very similar block copolymer, PS–PEO. The difference from our system is the solvent cyclopentane which is a nonsolvent for PEO and a $\theta$ solvent for polystyrene. In toluene we have good solvent conditions for both materials and no micelle formation for all concentrations employed. The affinity of the PEO block to the surface is largely due to H-bridging bonds to surface hydroxyl groups.[19] The adsorbed block copolymer can be rapidly displaced by injecting a PEO oligomer with a length comparable to the PEO block in the block copolymer (Figure 4c). The block copolymer is removed from the surface and a thin layer of the PEO oligomer is formed. This process is irreversible. Characterization in air leads to a refractive index of $n$(PEO) = 1.48 and layer thickness of $d_1 = 13$ Å. Thus, it is evident that PEO adsorbs in a rather flat conformation, as is known for the polar solvent water.[19] In a rather flat conformation, the adsorption energy is maximized.

With the block copolymer this adsorption energy gain is partially compensated by the PS block, which does not adsorb at the surface. The adsorption of PEO is thus favored over the adsorption of PS–PEO when PEO has in both cases the same molecular weight, thus leading to the displacement of the block copolymer by the PEO homopolymer.

**3.1. Adsorption Kinetics.** One qualitative feature of all measurements is that the amount of the adsorbed polymer increases monotonically with time and reaches a plateau value. Our data reveal two processes on a clearly separated time scale.

In the early stages, the time behavior of the adsorption can be described as a diffusion-controlled process. In the beginning ($t = 0$) we have an uncovered substrate at the position $x = 0$ and a solution with a well-defined homogeneous concentration $c_0$. The coordinate $x$ is perpendicular to the surface. We assume that each macromolecule reaching the surface is immediately adsorbed. In other words, the surface is regarded as a perfect sink for each polymer. These assumptions can be expressed by the following boundary conditions for the concentration:

$$c(x = 0,t) = 0 \qquad c(x,t = 0) = c_0 \tag{4}$$

The concentration profile due to the described perfect adsorbing wall can be evaluated by solving Fick's second law.

$$\frac{\partial c(x,t)}{\partial t} = D\frac{\partial^2 c(x,t)}{\partial x^2} \tag{5}$$

$D$ is the diffusion coefficient of the polymer in solution. A solution that takes the boundary conditions of eq 4 into account is

$$c(x,t) = c_0 \operatorname{erf}(x/2\sqrt{Dt}) \tag{6}$$

The error function erf is defined by

$$\operatorname{erf}(z) = \frac{2}{\sqrt{\pi}} \int_0^z e^{-x^2}\, dx \tag{7}$$

The flux $j$ to the surface is determined by the derivative of the concentration profile at $x = 0$ according to Fick's first law.

$$j(x = 0,t) = D\frac{\partial c(x = 0,t)}{\partial t} = \frac{Dc_0}{\sqrt{D\pi t}} \tag{8}$$

The integration of the flux with respect to $t$ leads to an expression of the adsorbed amount at the surface as a function of time.

$$A(t) = 2/\sqrt{\pi} c_0 \sqrt{Dt} \tag{9}$$

In the case of the absence of any convection, eq 9 should be the upper limit for the time dependence of the adsorbed amount. We have carefully avoided convection in our experiments. The rearrangement of chains at the uncovered surface is regarded to be fast compared to the necessary diffusion time in solution. One has to point out that eq 9 has no adjustable parameters. The diffusion coefficient can be measured by dynamic light scattering or obtained from the known hydrodynamic properties of PS in toluene. In Figure 5 the adsorbed amount for similar concentrations of the three PS–PEO samples is plotted versus $\sqrt{t}$. The dashed line is the adsorbed amount calculated according to eq 9. The diffusion coefficients obtained from our experiments with the use of eq 9 are listed in Table II. They are consistent with extrapolated literature data of diffusion coefficients of PS under similar conditions.[20] The uncertainty in the absolute concentration values at concentrations smaller than 0.01 mg/mL increases due to adsorption on the inner surfaces of the cell.

Equation 9 decribes the time behavior of the adsorption correctly until a certain coverage is reached. Knowing the maximum amount where eq 9 is valid we can calculate the interspacing distance $R_{\text{diff}}$ of the anchoring blocks (listed in Table II). The calculated values are between the radius of gyration $R_g$ and the end-to-end vector $r$ of

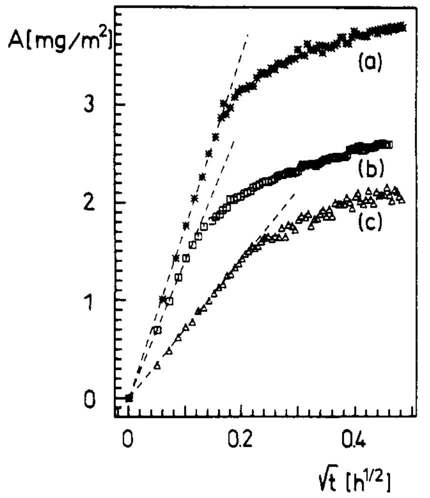

**Figure 5.** Absorbed amount of block copolymer as a function of adsorption time $t$ at the initial stages. (a) PS–PEO-80, (b) PS–PEO-184, (c) PS–PEO-502. All concentrations are similar ($c$ = 0.015 mg/mL); the dashed lines indicate the calculated $\sqrt{t}$ increase of the adsorbed amount, assuming that each molecule reaching the surface is adsorbed. No adjustable parameters are used for these calculations (for details, see text).

**Table II**
**Diffusion Constants and Molecular Parameters of PS–PEO**[a]

| sample | $D$, $10^{-7}$ cm$^2$/s | $R_g$, Å | $r$, Å | $R_{\mathrm{diff}}$, Å | $R_{\mathrm{int}}$, Å |
|---|---|---|---|---|---|
| PS–PEO-80 | 4.91 | 79 | 195 | 90 | 65 |
| PS–PEO-184 | 3.35 | 120 | 296 | 155 | 110 |
| PS–PEO-502 | 1.75 | 199 | 488 | 290 | 185 |

[a] $D$ are the diffusion coefficients obtained from a fit to eq 9, $R_g$ is the radius of gyration, $r$ is the end-to-end distance of PS in toluene, and $R_{\mathrm{diff}}$ and $R_{\mathrm{int}}$ are the calculated interspacing distances of the anchoring blocks in the diffusion-controlled regime and the plateau of the isotherms, respectively.

the unpertubed chains in solution. Equation 9 is therefore only valid until a surface coverage with little interaction of the adsorbed macromolecules is reached.

To obtain an indication of the chain conformation during the initial stages of the adsorption we have performed force balance measurements at a low concentration ($c$ = 0.003 mg/mL) for PS–PEO-184 (Figure 6). At this concentration the surface is not fully covered and the adsorbed amount is comparable to the adsorbed amount reached in the diffusion-controlled regime. Details of the experiments are described in ref 14.

The measured surface coverage in the diffusion-controlled regime is much lower than the coverage measured at infinite times. To get a still denser surface coverage, a penetration of a chain through the existing monolayer combined with conformational rearrangement to a more brushy conformation has to take place. This process is much slower than the time dependence in the diffusion-controlled regime. The increase of the adsorbed amount in the plateau region can be described by an exponential time behavior, which is evident from Figure 7, where ln ($A_\infty - A(t)$) is plotted versus the time in hours.

$$A(t) = A_\infty(1 - e^{-kt}) + \tilde{A} \qquad (10)$$

$A(t)$ is the adsorbed amount as a function of time leading to an asymptotic plateau value $A(t \rightarrow \infty) = A_\infty$. The exponential law holds after an adsorbed amount of $\tilde{A}$ is reached. The rate constant $k$ is given by the slope of the straight line for longer times in Figure 7. It is evident that both processes are on a widely separated time scale and we get a distinct crossover.

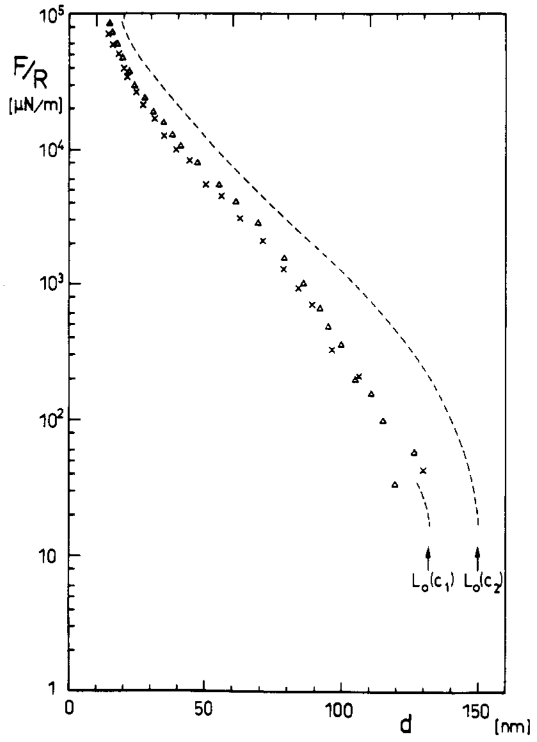

**Figure 6.** Force–distance profile of PS–PEO-184 measured at a concentration of 0.003 mg/mL and 21 ± 1 °C compared to the force–distance profile at full coverage, 0.1 mg/mL (dashed line).[28] Two compressions are shown (different symbols). The mean radius of curvature of the mica surface was 1.0 cm.

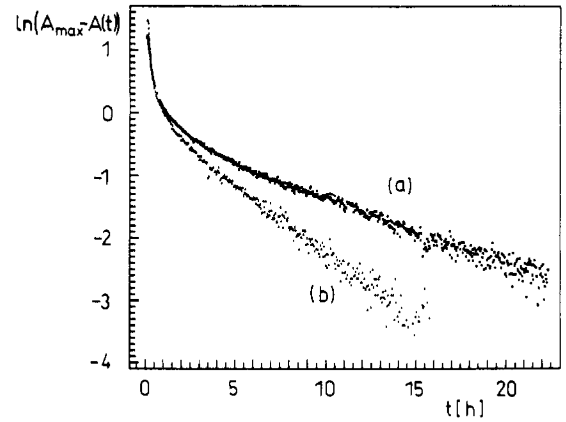

**Figure 7.** Long-time behavior of the adsorption. $A_\infty$ is the adsorbed amount at infinite times. (a) PS–PEO-502, (b) PS–PEO-184. All concentrations are similar (0.015 mg/mL). In the early stage, we observe the $\sqrt{t}$ behavior. Clearly distinct time behavior is observed at longer times. The increase of the adsorbed amount for longer times can be described by an exponential law. The calculated slopes for different concentrations are plotted in Figure 10.

**3.2. Adsorption Isotherm.** The adsorption isotherm is plotted in Figure 8. The adsorbed amount decreases with increasing length of the nonadsorbing PS part, keeping the length of the adsorbing PEO block constant. The adsorption isotherms show a broad plateau value.

There is no evidence of multilayer adsorption since at higher concentrations of the solution the adsorbed amount remains constant. The interspacing distance $R_{\mathrm{int}}$ of the anchoring blocks is calculated from the maximum adsorbed amount and is listed in Table II. Obviously the calculated values are significantly smaller than the end-to-end vector, indicating that the macromolecule is in an elongated conformation.

At very low concentrations we observe an indication of another plateau at approximately $A$ = 2.5 mg/m$^2$ for PS–

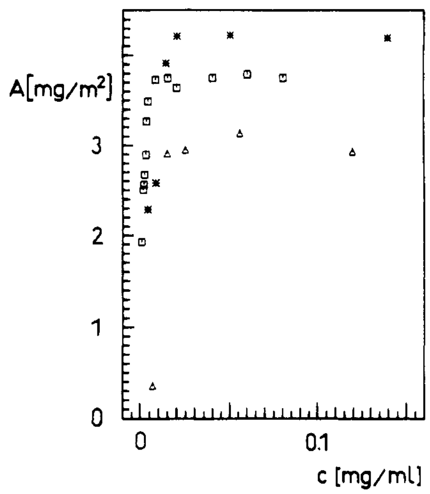

**Figure 8.** Adsorption isotherm of PS–PEO block copolymers of different molecular weight. (*) PS–PEO-80, (□) PS–PEO-184, (△) PS–PEO-502.

PEO-184. This is especially evident in a logarithmic plot of the isotherm. Since those concentrations are below 0.008 mg/mL, which is extremely dilute, we are, however, not completely sure whether other processes dominate the results. Therefore we do not discuss those data in detail here. For instance, competitive adsorption from other surfaces in the cell, uncertainty in the concentrations, and changes of the concentrations of the solution during the adsorption process might influence the results in this concentration region. Those effects do not play an important role at higher concentrations during our experiments.

## 4. Discussion

From our data we obtain the following picture of the adsorption process. Our kinetic data reveal a two-stage process on a clearly separated time scale. In the beginning, the time behavior of the adsorption is governed by diffusion of polymers to the surface. As soon as a block copolymer reaches the surface it will be anchored to the surface via the small PEO block. Internal rearrangement processes to adopt a favorable conformation for the adsorption with the PEO portion in the outer shell of the sphere are much faster than the transport to the surface. This assumption is reasonable comparing internal relaxation times with diffusion times of molecules, which are different by orders of magnitude. This is especially true in a good solvent for both components since no specific interaction of the solvent to the different blocks is present. One therefore does not expect thermodynamic effects on the conformation in solution. Similarly, with micelle formation the situation might be significantly different, which, however, has been excluded in our experiments by dynamic light scattering.

The PEO is adsorbed due to the affinity to surface hydroxyl groups and is expected to adopt a flattened conformation to maximize the adsorption energy. This picture is consistent with the displacement adsorption data, which prove very thin layer formation by the oligomers of PEO of similar molecular weight as compared to the PEO block in the block copolymers.

A schematic picture of the adsorption process is shown in Figure 9. Initial stages of adsorption are shown in Figure 9a, where only a dilute layer of adsorbed chains is present. At the very initial stages the chain conformation might be largely unperturbed despite the effect of the surface. To a first approximation one can assume that every molecule reaching the surface is directly adsorbed. Thus, a first coverage of the surface is formed where the adsorption is limited by the diffusion rate of chains to the surface and where the arrangement processes of chains at the surface to adopt a favorable conformation for adsorption is fast compared to the necessary diffusion times. The surface coverage is still low and chains arriving at the surface usually do not hit an already occupied site. Similarly, the desorption rate is low and the concentration in solution does not change significantly during adsorption. The adsorption rate is thus merely controlled by the diffusion process of chains to the surface. This picture is supported by (a) the $\sqrt{t}$ dependence of the adsorption rate, (b) the agreement of the diffusion coefficient used to fit the adsorption data based on eq 9 with those reported for chains in solution, (c) the approximate minimal area per molecule on the surface calculated from the deviation point from the $\sqrt{t}$ dependance, and (d) the indication of a first plateau level in the isotherm. We assume that the chain conformation at the surface in this $\sqrt{t}$ region is largely unperturbed with respect to the solution.

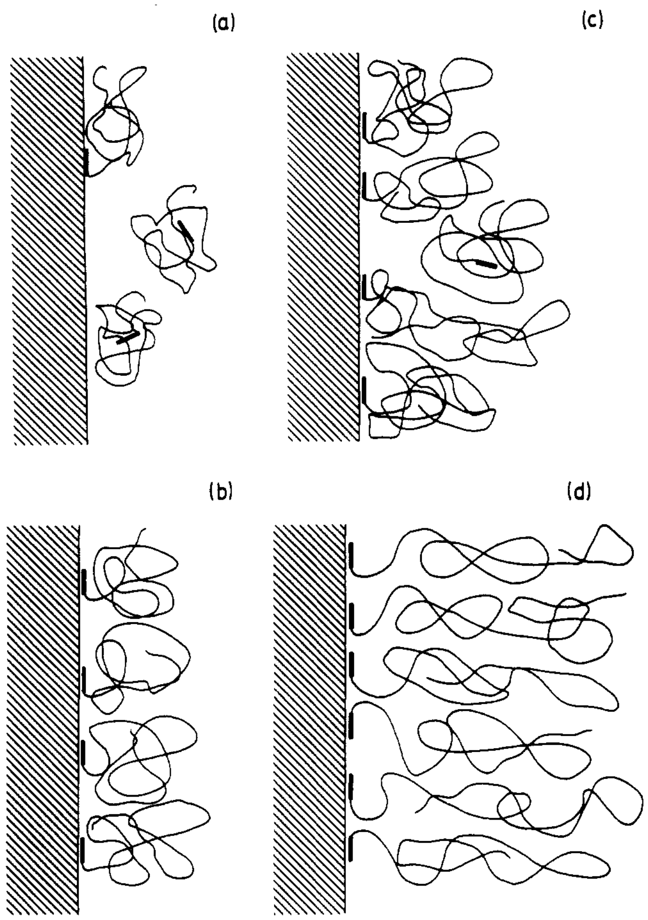

**Figure 9.** Schematic model for the adsorption process of a block copolymer with one adsorbing block on a solid wall. (a) Diffusion-controlled regime with low interaction of the molecules; (b) a complete monolayer has formed; (c) penetration of a molecule through the layer combined with conformational rearrangement; (d) brushlike chain conformation at final coverage.

To obtain an indication of the chain conformation in the transport-controlled regime, one can compare the mean distance between molecules at the surface $R_{\mathrm{diff}}$ with the characteristic dimensions of the chain in solution. This characteristic dimension is expressed by the radius of gyration $R_g$ or the end-to-end distance $r$ given in Table II. For all investigated block copolymers $R_{\mathrm{diff}}$ has a value between $R_g$ and $r$, indicating a close packing of chains as shown in Figure 9b. One can conclude that the chain conformation of adsorbed chains is not significantly distorted in this regime.

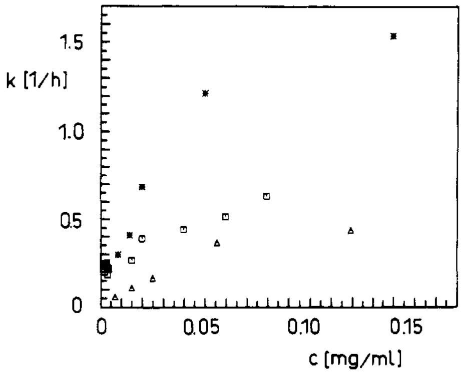

**Figure 10.** Rate constants $k$ of the long-time behavior as a function of concentration $c$. (*) PS–PEO-80, (□) PS–PEO-184, (△) PS–PEO-502.

A further insight into the conformation of the chains is given by the force–balance experiments carried out at a concentration of 0.003 mg/mL. According to our adsorption isotherm, the surface coverage (2.5 mg/m$^2$) is then between the maximum adsorbed amount (3.7 mg/m$^2$) and the transport limited value (1.7 mg/m$^2$). The force–distance profile indicates the following features: (a) there is no hysterisis for compression and decompression indicating a reversible conformation change as well as no evidence for bridging for the nonadsorbing PS portion, (b) the curve is shifted to lower distances compared to force diagrams obtained at higher concentrations, (c) the onset of the force $L_0$ starts at 130 nm as compared to 150 nm for the more concentrated solution, and (d) the form of the curve can be fitted with a brushlike conformation,[14] i.e., either a parabolic or a step function density profile, and is not consistent with a mushroomlike conformation of adsorbed chains. For adsorption in this region we thus already observe a distorted chain conformation toward a brush. Experiments with the force–balance technique at still lower concentrations are difficult to perform.

The derived expression for transport-limited adsorption describes the time behavior in the early stages. At longer times (Figure 7) we observe significant deviations from the $\sqrt{t}$ dependence and can assume that chain rearrangement and deformation plays a major role. When a certain coverage is reached, the preformed layer is a barrier for further molecules to reach the surface. Each molecule has to overcome an osmotic pressure that increases with the average concentration of the adsorbed layer. With an increasing adsorbed amount the adsorbed molecules have to adopt an increasingly stretched brush conformation. The term brush conformation is used in the literature and by us when the interspacing distances of the anchoring blocks are significantly lower than the end-to-end distance. This is valid in our case at larger times, as seen in Table II. However, this does not imply that individual chains are completely stretched and the true situation is likely to be in between Figure 9b and d.

The final increase of the adsorbed amount can be described by an exponential law, eq 10. The dependance of the rate constant $k$ on molecular weight and concentration of the solution is plotted in Figure 10. The time needed to reach the asymptotic plateau value $A_\infty$ increases with the molecular weight, as seen by the values of the rate constant. For instance, PS–PEO-184 needs, at low concentrations, 2 days to reach the final value of the adsorbed amount. The rate constant $k$ increases at low concentrations linearly with the concentration $c$. At higher concentrations $k$ levels off with a further increase of the concentration. This process of adsorption at later times goes in the direction of more brushy conformation, as schematically shown in Figure 9c. A first adsorbed layer is already present and further chains have to penetrate this layer to achieve adsorption. This process needs rearrangement and deformation of already adsorbed chains. A molecule arriving from solution at the surface still can penetrate the adsorbed layer with a certain probability, at least partially, when for instance by conformational fluctuations a hole has emerged.

At this stage there is still a large probability that the penetrating chain will be pushed out again since the conformational changes involved largely discourage further penetration. In this much denser system as compared to early stages of adsorption, rearrangement times to achieve a favorable conformation for adsorption might also increase. The system is, however, still far from being dense and could be considered as semidilute. The gain in energy during adsorption compensates the loss in entropy due to the distorted chain conformation. Thus a maximal surface coverage is achieved (Figure 9d) where further penetration of chains involves a conformation that is too strongly distorted to compensate against the energy gain during adsorption. The maximal adsorbed amount should thus increase with increasing PEO block length and decrease with increasing PS block length. Since in our case the size of the anchoring block is kept approximately constant while the size of the PS block is varied, the repulsive interaction between PS blocks determines the maximal adsorbed amounts. The short PEO blocks do not form a dense homogeneous layer at the surface. Even if one assumes a completely flat configuration of the PEO at the surface, there are a lot of free available surface sites left even when the maximum adsorbed amount is reached. Thus, in our case, with approximately constant PEO block length the nonadsorbing PS block determines the maximum adsorbed amount.

In addition, it is evident that smaller chains can penetrate the layer easier as compared to larger ones and the rate constant $k$ thus generally decreases with increasing molecular weight of the PS block at a given concentration. At the same time it initially increases with concentration $c$ of the solution since with increasing $c$ statistically more molecules hit the surface. This corresponds to a Langmuir-type picture of adsorption of molecules through the preformed layer. The rate constant $k$ of the exponential expression derived from the Langmuir model depends linearly on the concentration, $k = k_1c + k_2$. Here $k_1$ is the adsorption rate and $k_2$ the desorption rate. Since the desorption of chains, for instance, after replacement of the polymer solution by pure toluene, is not observed one can conclude that the desorption rate $k_2$ is small, leading to a linear expression of the rate constant $k$ on the concentration $c$. This simple picture seems to explain the adsorption kinetics at smaller concentrations and at later stages rather well. At higher concentrations we observe deviations from the linear behavior. A further increase in the concentration does not increase the adsorption rate. One might assume that in this region the rearrangement of chains in the layer and diffusion through the layer becomes the limiting factor for adsorption.

On a molecular level the processes involved are supposed to be fairly complicated. Using the reptation-like picture for the interpenetration of chains,[21] one can derive a "quasi-logarithmic" regime at intermediate times and an exponential regime at later times.[23] In our experiments we observe only the latter regime.

The adsorption is irreversible with respect to a change of the solution against pure toluene. We do not observe a change in the adsorbed amount within 1 day when the

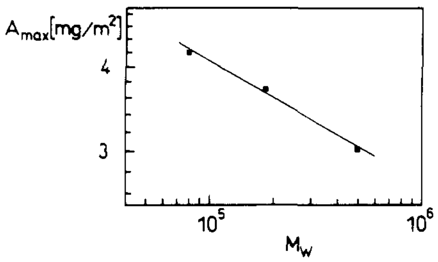

**Figure 11.** Maximal adsorbed amount $A_{max}$ as obtained from the plateau values of the isotherm as a function of the molecular weight $M_\omega$. The solid line corresponds to a $M_\omega^{-0.18}$ power law.

solution is replaced with pure toluene. The maximum adsorbed amount at long times decreases with increasing lengths of the nonadsorbing tail. A double-logarithmic plot of the adsorbed amount $A_{max}$ via the molecular weight is given in Figure 11. The straight line corresponds to a $M_\omega^{-0.18}$ power law. This behavior is consistent with the assumption that the adsorbed amount depends on the volume that each molecule occupies. Adsorption is favored by the energy gain due to the interaction of the PEO block with the surface while entropic and steric effects hinder further adsorption.

## 5. Conclusion

The kinetics of adsorption of block copolymers from dilute solution onto a solid dielectric surface has been investigated by ellipsometry. The technique proves to be very sensitive for the adsorbed amount of block copolymer irrespective of the detailed nature of the profile. Block copolymers used can be regarded as end-functionalized chains since under the good solvent conditions only the small PEO block adsorbs strongly to the surface while the larger PS block does not.

The system studied is a remarkable example of self-assembling of polymers. Although we start adsorption runs at a bulk polymer concentration of 0.01 mg/mL, the average polymer concentration in the adsorbed layer is ~100 mg/mL.

The kinetics of adsorption can be described by a two-stage process. Process 1 is the formation of a first monolayer with low interaction between the molecules. Adsorption is limited by the diffusion process of chains to the surface while internal chain rearrangement during adsorption is much faster and does not play a significant role in the adsorption kinetics. With progressing time, interactions between chains become important and the adsorption process slows down. A first surface layer with still little interaction between chains is formed. Further adsorption can only proceed via further deformation of chains forming an increasingly brushlike conformation. Since in our case the energy gain by adsorption of PEO blocks on the surface is only small because of the small size of the PEO block the chain deformation is not extremely large and maximal surface coverage is limited by the repulsive interaction of PS blocks.

We do observe, however, two clearly distinct time regimes corresponding to, first, the diffusion-limited adsorption process and, second, the slowing down caused by the slow penetration process of chains through the activation barrier formed by the already adsorbed chains. Rate constants can be explained on the basis of solution diffusion coefficients and Langmuir theory, respectively. In connection with force–balance experiments[14] performed on the same polymers, a fairly complete picture of the adsorption process of end-functionalized polymers on a solid surface from good solvent conditions is achieved.

**Acknowledgment.** We gratefully acknowledge the help of Dr. M. Schmidt and Dr. M. Aven during the dynamic light scattering experiments and of Dr. M. A. Ansarifar during the force balance measurements.

## References and Notes

(1) Lee, L. H. *Adhesion and Adsorption of Polymers*; Plenum Press: New York, 1980.
(2) Napper, D. H. *Polymeric Stabilisation of Colloid Dispersions*; Academic Press: London, 1975.
(3) Ruckenstein, E.; Chang, D. B. *J. Colloid Interface Sci.* **1988**, *123*, 170.
(4) Silberberg, A. *J. Phys. Chem.* **1962**, *66*, 1872.
(5) DiMarzio, E. A. *J. Phys. Chem.* **1965**, *42*, 2101.
(6) Chan, D. *J. Chem. Soc., Faraday Trans.* **1975**, *71*, 235.
(7) Lax, M. *Macromolecules* **1974**, *7*, 660.
(8) Feigin, R. I.; Napper, D. H. *J. Colloid Interface Sci.* **1979**, *71*, 117.
(9) Takahashi, A.; Kawaguchi, M. *Adv. Polym. Sci.* **1982**, *46*.
(10) Alexander, S. *J. Phys.* **1977**, *38*, 983.
(11) de Gennes, P. G. *Macromolecules* **1980**, *13*, 1069.
(12) Millner, S. T.; Witten, T. A.; Cates, M. E. *Europhys. Lett.* **1988**, *5*, 413.
(13) Azzam, R. M. A.; Bashara, N. M. *Ellipsometry and Polarized Light*; North Holland Publication: Amsterdam, 1979.
(14) Taunton, H. J.; Toprakcioglu, C.; Klein, J. *Macromolecules* **1988**, *21*, 3336.
(15) Lekner, J. *Theory of Reflection*; Martinius Nijhoff: Dordrecht, The Netherlands.
(16) Dolan, A. K.; Edwards, S. F. *Proc. R. Soc., London* **1975**, *A343*, 427.
(17) Mac Crackin, F. L.; Passaglia, E.; Stromberg, R. R. *J. Res. Natl. Bur. Stand., Sect. A* **1963**, *67A*, 363.
(18) Cogan, K. A.; Gast, A. P. *Macromolecules* **1990**, *23*, 745.
(19) Killmann, E.; Wiegand, H. G. *Makromol. Chem.* **1970**, *193*, 132.
(20) Brandrup, J.; Immergut, E. H. *Polymer Handbook*; John Wiley & Sons: New York, 1989.
(21) Halperin, A.; Alexander, S. *Europhys. Lett.* **1988**, *6*, 329.
(22) Förster, S.; Schmidt, M.; Antonietti, M. *Polymer* **1990**, *31*, 781.
(23) Ligoure, Ch.; Leibler, I. *J. Phys. F.* **1990**, *51*, 1313.
(24) Tassin, J. F.; Siemens, R. L.; Tang, W. T.; Hadziioannou, G.; Swalen, T. D.; Smith, B. A. *J. Phys. Chem.* **1989**, *93*, 2106.
(25) Munch, M. R.; Gast, A. P. *Macromolecules* **1990**, *23*, 2313.
(26) Taunton, H. J.; Toprakcioglu, C.; Fetters, L. J.; Klein, J. *Macromolecules* **1990**, *23*, 571.

**Registry No.** (PS)(PEO) (block copolymer), 107311-90-0; PEO (SRU), 25322-68-3; toluene, 108-88-3.